



Dosimetric impacts of cone-beam computed tomography (CBCT)-based anatomic changes in intensity-modulated radiotherapy for cervical cancer

Han Yang^{1^}, Xiujuan Zhao², Yang He¹, Xia Tan¹, Haiyan Peng¹, Mingsong Zhong¹, Qicheng Li¹, Xianfeng Liu¹, Yanan He¹, Huanli Luo¹, Fu Jin¹

¹Department of Radiation Oncology, Chongqing University Cancer Hospital, Chongqing, China; ²Department of Gynecological Oncology, Chongqing University Cancer Hospital, Chongqing, China

Contributions: (I) Conception and design: H Yang, H Luo, F Jin; (II) Administrative support: H Luo, F Jin; (III) Provision of study materials or patients: H Luo, X Zhao, Y He, H Peng, X Tan; (IV) Collection and assembly of data: H Yang, M Zhong, Q Li, X Liu, Y He; (V) Data analysis and interpretation: H Yang, H Luo, F Jin; (VI) Manuscript writing: All authors; (VII) Final approval of manuscript: All authors.

Correspondence to: Huanli Luo. Department of Radiation Oncology, Chongqing University Cancer Hospital, 181 Hanyu Road, Shapingba District, Chongqing 400030, China. Email: guyexianxue@126.com; Fu Jin. Department of Radiation Oncology, Chongqing University Cancer Hospital, 181 Hanyu Road, Shapingba District, Chongqing 400030, China. Email: jfazj@126.com.

Background: To evaluate the effects of dose to tumors and organs at risk (OARs) on inter-fractional anatomic changes.

Methods: We evaluated nine patients with cervical cancer treated with intensity-modulated radiotherapy (IMRT) (45 Gy in 25 fractions) using kV cone-beam computed tomography (CBCT) image guidance once or twice a week before treatment. For each patient, the original plan on the computed tomography (CT) image was copied to merged images, and then the fractional doses were calculated. Subsequently, deformable accumulated doses were obtained by summing the fractional absolute doses into a single dose in MIM Maestro software. The volume changes in the target and OARs were compared between the original CT and merged CBCT images, and the differences in the fractional and accumulated doses were also evaluated.

Results: Sixty-nine merged CBCT images were obtained and analyzed in this study. For the target areas, the volume changes in the clinical target volume (CTV) and planning target volume (PTV) reached -18.05% and -24.11% at most, respectively. The fractional $D_{2\%}$ of the CTV and PTV was generally higher than the original plans, and the accumulated deviations were $2.27\% \pm 0.82\%$ ($P < 0.01$) and $2.42\% \pm 1.28\%$ ($P < 0.01$), respectively. The fractional $D_{98\%}$ of the PTV was underdosed up to 18.28% for 78% of patients, and the accumulated deviations were -2.06% to -17.29% ($P < 0.05$). For the OARs, the bladder volume changes were the most dramatic, reducing up to 93.60%. The fractional D_{mean} and D_{2cc} of the bladder were generally higher than the original plans, and there were significant differences in their accumulated values ($P < 0.05$). There was no obvious trend of rectal volume change with -69.65% to 74.20%. The rectum D_{mean} and D_{2cc} of the accumulated were not significantly different from the planned dose ($P > 0.05$).

Conclusions: For patients with cervical cancer, the changes in bladder and rectal volume were greater than in the target volume. Although the volume changes in the bladder and rectum had no significant effect on $D_{98\%}$ of the CTV and PTV, they had a significant effect on their own D_{2cc} and the $D_{2\%}$ of the CTV and PTV. More attention should be paid to the volume changes in the bladder and rectum in clinical work.

Keywords: Merged cone-beam computed tomography image (merged CBCT image); CBCT-based dose calculation; anatomic changes; deformation dose; dosimetric uncertainties

[^] ORCID: 0000-0002-9988-3880.

Submitted Nov 25, 2022. Accepted for publication Dec 19, 2022.

doi: 10.21037/atm-22-6157

View this article at: <https://dx.doi.org/10.21037/atm-22-6157>

Introduction

Intensity-modulated radiotherapy (IMRT) is an advanced three-dimensional irradiation technology developed in the past 20 years. It is capable of creating highly conformal dose distributions with sparing of normal tissues and have been widely used in cervical cancer radiotherapy (1). It has been reported that IMRT can reduce the dose received by the bladder, rectum, and small intestine during adjuvant radiotherapy after radical hysterectomy for cervical cancer. It can also significantly reduce gastrointestinal and urinary complications and hematological adverse reactions, and improve the tumor control rate and survival status of patients (2,3). However, anatomic changes (such as the different filling status of the bladder and rectum) during the treatment course are one of the leading contributors of delivered dose uncertainties in radiotherapy, potentially causing underdosage to the targets or overdosage to organs at risk (OAR) relative to the planned dose distribution (4-6). Therefore, it is meaningful to apply image-guided radiation therapy (IGRT) and adaptive radiotherapy (ART) (7-9).

Cone-beam computed tomography (CBCT) either a kilovoltage beam delivered using an additional x-ray tube

mounted on the linac, to image the object from multiple projection angles and reconstruct a 3D image using the projected images. CBCT improves the repeatability of patient positioning compared with conventional two-dimensional image guidance (10). But the matching of planning CT and CBCT images cannot fully reflect the anatomical changes of all organs simultaneously. Therefore, some scholars have explored the dosimetric changes caused by the volume and morphological changes of the target and OARs based on CBCT image dose calculation in cervical and pancreatic cancer radiotherapy (11). Unfortunately, the limited field of view (FOV) range of the CBCT hardware equipment cannot contain all the information about the target and OARs in cervical cancer radiotherapy, and the areas beyond the range of CBCT can only be simulated by the original image registration. Image stitching provides a good method to solve this problem.

In this study, we combined three CBCT images to generate a merged image with a scan length of 46 cm. This image can cover the entire pelvic cavity and contains all the information about the target and OARs in radiotherapy for cervical cancer. Subsequently, the changes in volume during treatment and their effect on the fractional and accumulated dose were analyzed for the target and OARs on merged CBCT images. The inter-fractional morphological changes in organs were also observed. According to our literature review, studies on the effect of volume change on fractional dose and accumulated dose in treatment using image stitching are currently scarce. We present the following article in accordance with the MDAR reporting checklist (available at <https://atm.amegroups.com/article/view/10.21037/atm-22-6157/rc>).

Highlight box

Key findings

- We found that if the volume of the bladder and rectum were not strictly controlled in the radiotherapy of patients with cervical cancer, their changes were very large. It could significantly increase the CTV $D_{2\%}$, and it will also have a significant impact on the bladder and rectum's own D_{2cc} .

What is known and what is new?

- Anatomic changes during the treatment course are one of the leading contributors of delivered dose uncertainties in radiotherapy.
- In this study, we combined three CBCT images which can cover the entire pelvic cavity and contains all the information about the target and OARs in radiotherapy for cervical cancer.

What is the implication, and what should change now?

- The merged CBCT data in this study provides a suitable approach in ART that may be useful clinically to respond to the daily anatomy variations in cervical cancer patients.

Methods

Patient population

This study included nine patients with stage IA1–IIIC1r cervical cancer (International Federation of Gynecology and Obstetrics) who received IMRT in the Chongqing University Cancer Hospital. Of these, four patients underwent radical hysterectomy, four received lymph node dissection, and one did not have surgery. The basic

Table 1 Patient information

Patient ID	Age (years)	Height (cm)	Weight (kg)	Histology and stage	Surgery	Adjuvant treatment
1	66	142	52	Squamous cell carcinoma IA1	Radical hysterectomy	Concurrent chemoradiotherapy
2	28	160	46.5	Adenosquamous cell carcinoma IB2	Radical hysterectomy	Concurrent chemoradiotherapy
3	50	155	59	Squamous cell carcinoma IIC1p	Lymph node dissection	Concurrent chemoradiotherapy
4	56	153	51	Adenocarcinoma IB	Radical hysterectomy	Concurrent chemoradiotherapy
5	76	155	50	Squamous cell carcinoma IIIB	None	Concurrent chemoradiotherapy
6	53	155	51	Squamous cell carcinoma IIC1r	Lymph node dissection	Concurrent chemoradiotherapy
7	59	155	61	Squamous cell carcinoma IIC1p	Lymph node dissection	Concurrent chemoradiotherapy
8	35	158	54	Squamous cell carcinoma IIA1	Radical hysterectomy	Concurrent chemoradiotherapy
9	51	155	61	Squamous cell carcinoma IIC1r	Lymph node dissection	Concurrent chemoradiotherapy

information about these patients is summarized in *Table 1*. None of the patients had radiotherapy contraindications, and all voluntarily underwent merged CBCT scans once or twice weekly. The study was conducted in accordance with the Declaration of Helsinki (as revised in 2013). This study was approved by the Ethics Committee of Chongqing University Cancer Hospital (No. CZLS2021048-A) and informed consent was taken from all the patients.

Positioning and contouring

All patients were placed in the supine position with both hands raised and fixed with a thermoplastic membrane. Half an hour before the positioning scan, the patients were instructed to empty their bladders and then drink 250 mL of water. No instructions on rectal filling were given to these patients. The computed tomography (CT) scanning (Big Bore; Philips Brilliance, Holland) was performed for each patient at 5 mm slice thickness with a scope from the diaphragm level to 4 cm below the ischial tubercle. The CT images were imported to the Eclipse treatment planning system (TPS) (Varian Medical Systems, Version 15.6, Inc., USA) and prepared for contouring.

The target and OARs were delineated by the same experienced radiation oncologist according to the International Commission on Radiation Units and Measurement (ICRU) Report 62. The clinical target volume (CTV) of the pelvic cavity included the whole uterus (if present), the vaginal stump, 1/2 of the upper segment of the vagina, the parauterine/paravaginal soft tissue, the pelvic lymphatic drainage area (including the common iliac,

external iliac, internal iliac, obturator, and presacral lymph node areas), the upper boundary to the level of the 4th to 5th lumbar vertebrae, and the lower boundary to the lower edge of the obturator. The planning target volume (PTV) was generated from the CTV, adding a 5 mm margin with all expansion to offset setup uncertainties. Then, the small intestine, rectum, bladder, and femoral head were contoured as the OARs. Among them, the small intestine included the intestinal tube and its surrounding mesenteric tissue; the upper boundary of the rectum was the junction of the rectum and the sigmoid colon, and the lower boundary was the anus. The contour of the bladder reflects its filling state.

Treatment planning

The IMRT plans for all patients were designed on the Eclipse TPS with 6 MV photon beams generated by an EDGE linear accelerator with a Millennium 120 MLC (Varian Medical Systems). The IMRT plans contained seven co-planar fields (210°/260°/310°/0°/50°/100°/150°). The dose prescribed to the PTV was 45 Gy in 25 daily fractions. The planning goal was to achieve 95% or more of the PTV receiving the prescription dose, with the maximum dose point not exceeding 110% of the prescription dose. The dose constraints of the OARs were based on the Radiation Therapy Oncology Group-1203 Randomized Phase III trial guidelines.

In all plans, photon optimizer (PO) algorithms were used for optimizations, and the anisotropic analytical algorithm (AAA) was applied for the final dose calculations. The resolution used for the dose calculation was 2.5 mm in all

directions. The maximum speed of the multi-leaf collimator (MLC) motion was 2.5 cm/s. In addition, the jaw tracking method was also used. In this method, the jaw moves with the changes in MLC position in real-time while the beam is on. This technique reduces the opening size of the jaw as much as possible to minimize transmission and leakage, thus reducing the normal tissue dose (12-14).

Image acquisition and merging

All patients underwent CBCT scans prior to treatment once or twice a week using a Varian On-board Imager Spotlight protocol. The scanning parameters were as follows: 360° rotation scan, 120 kV, FOV 26 cm in diameter, and 5 mm slice thickness. For each image guidance, we collected three CBCT images; one on the planning center, which was used for 3D matching, and the other two images generated on the 15 cm movement of the planning center in the direction of the advance and retreat bed. The area covered by both individual volumes was irradiated twice. This overlap led to visible artifacts in the border region between the two volumes. The image information in the overlapping area was processed and merged by keeping the brighter [more Hounsfield units (Hus)] voxel for each single voxel. Then, the merged images were obtained, which covered the entire pelvic cavity with a scan length of 46 cm.

Volume correction

The target and OARs on the merged CBCT images were delineated by the same experienced radiation oncologist, according to the ICRU Report 62. Nevertheless, there were still differences in artificial delineation caused by the influence of the CBCT image quality. To solve this problem, the humeral heads were used as a reference to correct the volume. The correction formula was as follows:

$$V_{\text{corrected}} = V_{\text{contour}} \times (1 + \Delta V_{\text{Femoral head}} / 100) \quad [1]$$

$$\Delta V_{\text{Femoral head}} = (\Delta V_{\text{Femoral head R}} + \Delta V_{\text{Femoral head L}}) / 2 \quad [2]$$

$$\Delta V_{\text{Femoral head R/L}} = (V_{\text{CBCT}} - V_{\text{CT}}) / V_{\text{CT}} \times 100 \quad [3]$$

Here, $V_{\text{corrected}}$ is the corrected volume; V_{contour} is the original contour volume; $\Delta V_{\text{Femoral head R/L}}$ is the volume deviation of the right or left femoral heads between each fractional merged CBCT and original CT image; $\Delta V_{\text{Femoral head}}$ is the mean volume deviation of the femoral heads; V_{CBCT} and V_{CT} are the volumes of the corresponding

structures in CBCT and CT, respectively.

For a more accurate dose calculation, the contour lines of the target and OARs on each merged CBCT image were corrected by calculating the equivalent spherical radius R_{contour} and $R_{\text{corrected}}$ before and after volume correction through V_{contour} and $V_{\text{corrected}}$. According to the difference between the two radii, the structures were placed outward or inward in the TPS.

CBCT-based dose calculation

Before CBCT-based dose calculation, a calibration of the HUs to electron density (ED) was performed for inhomogeneity corrections using the Advanced Electron Density Phantom Model 1467 (Gammex Inc., USA) (Figure 1A) (15). This phantom and its material insert were scanned with the standard clinical protocol (Figure 1B). The HU of each insert was extracted within a region of interest (ROI) and assigned to the known related relative ED to generate a calibration curve for the TPS (Figure 1C).

Subsequently, the merged CBCT images for each patient were matched onto the planning CT image according to the bony anatomy using 3D/3D matching. The original plan was copied to the merged CBCT image, and then the fractional delivered doses were calculated and compared with the original planned dose.

The calculation process of the CBCT-based accumulated delivered dose is presented in Figure 2, taking Patient 8 as an example. In this process, the status of the treatment fraction without CBCT scanning prior to treatment was replaced by the last merged CBCT image to simulate the daily treatment status of patients to the maximum extent. A free deformable image registration (DIR) algorithm (VoxAlign™) based on the image intensity from MIM Maestro was used to map the voxels (dose) from one merged image to another merged image. The sequence of dose accumulation by image registration (Figure 2) was to superimpose the 1st and 2nd CBCT doses onto the 2nd CBCT image, then superimpose the superimposed results with the 3rd CBCT dose onto the 3rd CBCT image, and so on. The final deformation accumulated dose was obtained.

The CBCT-based delivered doses were compared with the planned doses for each treatment day and the accumulated doses for the entire treatment. CTV $D_{98\%}$, CTV $D_{2\%}$, PTV $D_{98\%}$, PTV $D_{2\%}$, and D_{2cc} and D_{mean} of the OARs were compared between the original plan and actual accumulated delivery.

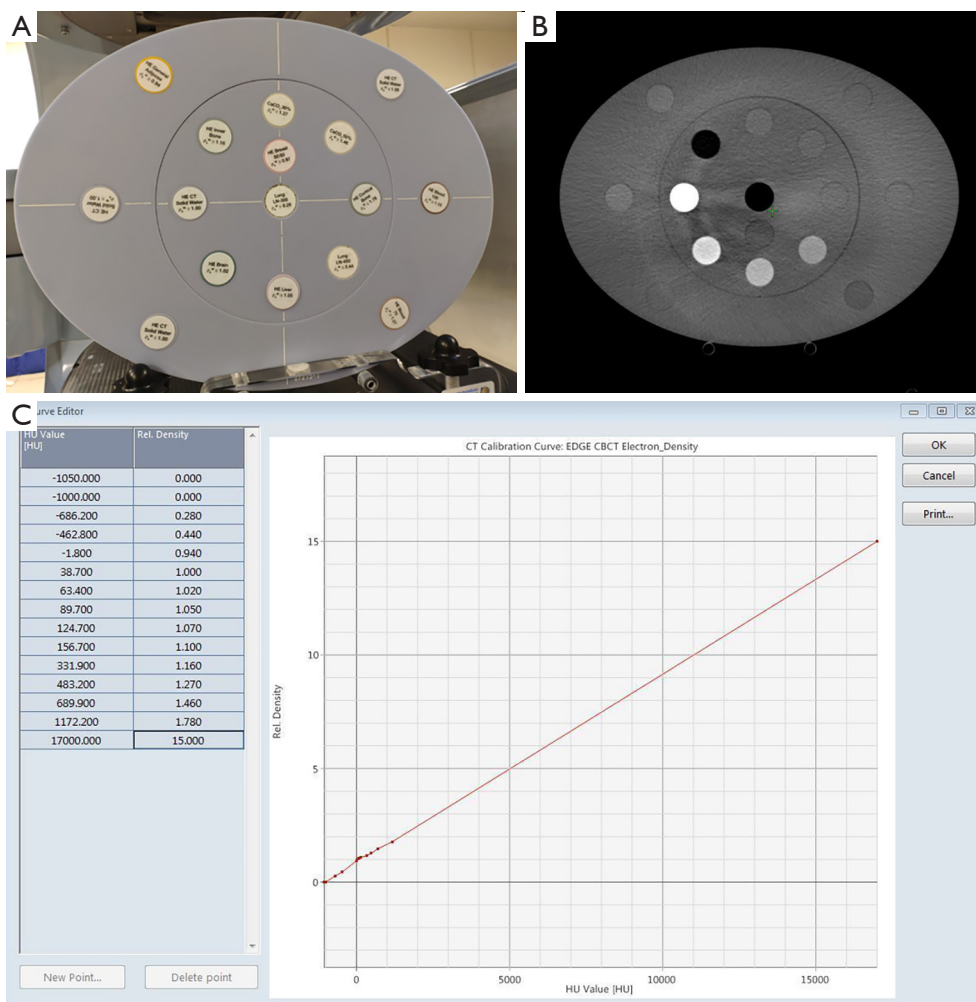


Figure 1 Hounsfield units to electron density calibration. (A) Advanced Electron Density Phantom Model 1467. (B) CBCT image for the phantom. (C) The calibration curve of HUs to ED. CBCT, cone-beam computed tomography; HUs, Hounsfield units; ED, electron density.

Statistical analysis

The paired differences in CTV, PTV, and OAR metrics were analyzed by comparing the planned and accumulated doses using SPSS 19.0 statistical software (SPSS, Chicago, IL, USA). According to the Shapiro-Wilk test, some data of the accumulated doses did not follow a normal distribution, so the data in this paper are represented by the median and upper and lower quartiles [M (P25, P75)]. The multi-sample nonparametric rank sum test was used, and the Kruskal-Wallis test was performed. The effect of volume change on the fractional dose was analyzed by Pearson correlation. A P value <0.05 was considered statistically significant.

Results

Fractional volume changes of the target and OARs

Sixty-nine merged CBCT images covering the entire pelvic cavity were obtained in this study. Compared with the original CT images, the fractional volume changes of the target and OARs are shown in *Figure 3A-3D*, and the statistical results are shown in *Table 2*. The differences made by manual delineation based on CBCT are shown in *Figure 3E* and *3F*, with a mean range from -2.36% to 0.93% .

In general, the results of the study were not affected by the patient's surgical status. The CTV and PTV volume

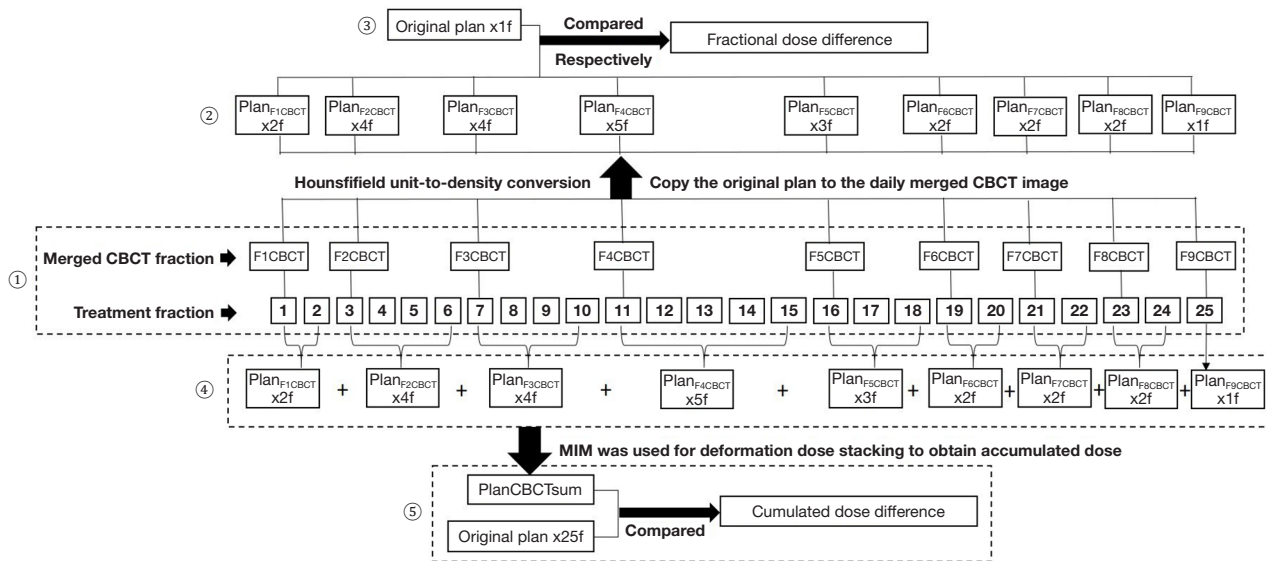


Figure 2 The calculation process of the CBCT-based accumulated delivered dose, taking Patient 8 as an example. CBCT, cone-beam computed tomography.

changes ranged from -24.11% to 4.29% . The most significant change was found in the bladder volume, and this reduction was as high as 93.60% , except for Patient 6. There was no significant trend in rectal volume, ranging from -69.65% to 74.20% . As an example, the contours of the target and OARs in each fractional merged CBCT image of Patient 2, mapped to the original CT by registration, are shown in *Figure 4*. For Patient 2, the bladder profile changed significantly in the sagittal plane compared with the coronal plane and cross-section, and the volume changes of the target and other organs were small.

Evaluation of merged CBCT-based fractional delivered dose

Figure 5 shows the fractional dose change of the CTV, PTV, bladder, and rectum for each patient during fractional treatment relative to the original plan. The statistical results are shown in *Table 2*. As shown in *Figure 5*, the fractional $D_{2\%}$ of the CTV and PTV was higher than the original plan, and the maximum was 4.52% . The average deviation of the CTV $D_{98\%}$ was -2.00% to 2.55% for all patients. Except for Patients 6 and 8, the fractional $D_{98\%}$ of the PTV was underdosed up to 18.28% . For the bladder, the fractional D_{mean} and $D_{2\text{cc}}$ were in most cases higher than the original plan. The average deviation of the rectum D_{mean} was -9.92% to 16.02% for all patients, and the changes on $D_{2\text{cc}}$ were -2.99% to 6.37% .

Evaluation of merged CBCT-based accumulated delivered dose

The differences between the target and OARs in the accumulated delivered doses and planned doses are shown in *Table 3* and *Figure 6*. The accumulated relative deviations on $D_{2\%}$ of the CTV and PTV were $2.27\% \pm 0.82\%$ ($P < 0.01$) and $2.42\% \pm 1.28\%$ ($P < 0.01$), respectively. For the dose coverage of the target, the CTV $D_{98\%}$ deviation was within -6.59% to 2.18% , and there was no significant difference ($P > 0.05$). Overall, the PTV $D_{98\%}$ was undervalued by 2.06% to 17.29% , and there was a statistically significant difference ($P < 0.05$). As shown in *Table 3*, the accumulated D_{mean} and $D_{2\text{cc}}$ of the bladder were significantly higher than the planned dose ($P < 0.05$), and there was no significant difference for the rectum accumulated D_{mean} ($P > 0.05$).

Effect of volume change on the fractional dose delivered

The effects of volume changes in the target and OARs on the fractionated delivered dose are shown in *Table 4*. The change in CTV volume only affected the dosimetric parameters of the PTV. The volume changes in the PTV had a greater effect on dose than the other three but did not have any effect on the rectal dose. Changes in the volume of the bladder and rectum had significant effects on their own $D_{2\text{cc}}$ and also had significant effects on the CTV $D_{2\%}$ and PTV $D_{2\%}$.

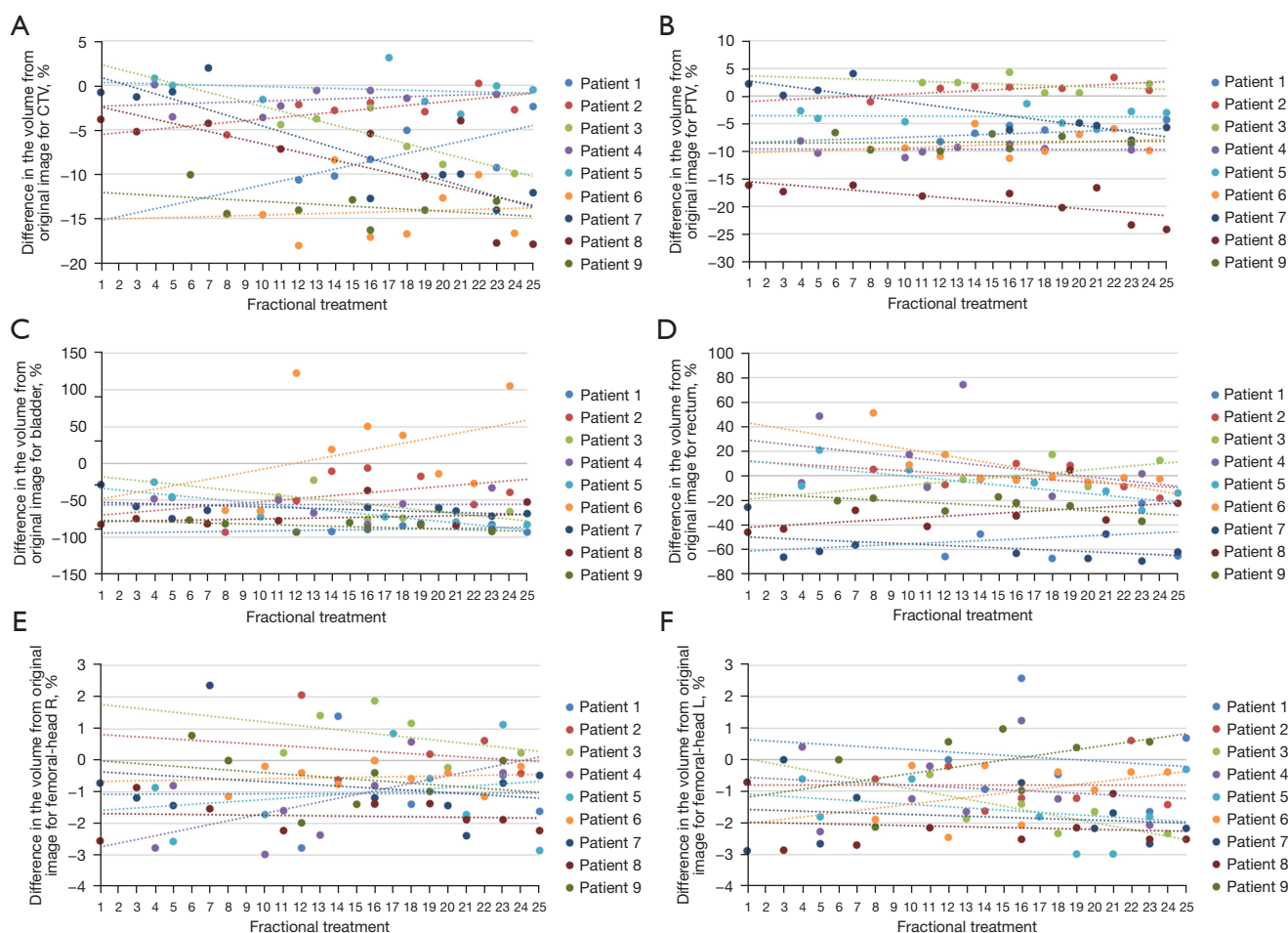


Figure 3 Fraction changes in the target and OARs during treatment: (A) CTV; (B) PTV; (C) bladder; (D) rectum; the differences made by manual delineation are shown in (E) and (F). The percentage of volume difference was calculated by the volume on merged CBCT images minus the original CT images and then divided by the volume on the original CT images. CTV, clinical target volume; PTV, planning target volume; OARs, organs at risk; CBCT, cone-beam computed tomography.

Discussion

In this study, the merged CBCT reflected the whole pelvic state of the patient during treatment. Dosimetric uncertainties are mainly caused by changes in the shape and volume of the patient's organs. We found that the fractional volumes of the CTV, PTV, bladder, and rectum were significantly different, which caused many patients to receive higher doses to the OARs. Moreover, both the fractional doses and the accumulated doses of the CTV and PTV were underdosed compared with the original plan.

The target area of external irradiation for cervical cancer is located in the abdominal and pelvic cavities. The target area positions are easily affected by the bladder-filling state

and intestinal movements (16-18). In this study, the patients emptied their bladders half an hour before positioning and drank 250 mL of water but did not strictly follow the doctor's instructions during the actual follow-up treatment. It can be seen from *Table 2* and *Figure 3* that the volume of the bladder and rectum changed greatly, reaching -90% and -70% , respectively, and their volumes changed mainly in the direction of head-to-foot and abdomen-to-back (*Figure 4*). The change in bladder volume was generally reduced except for Patient 6. This patient did not strictly follow the doctor's advice during localization, which led to insufficient bladder filling in the localization CT, contrary to other patients. Although the PTV is obtained by uniformly expanding the CTV by 0.5 cm, the volume

Table 2 The difference in volume and dose between merged CBCT images and original CT images

No.	CTV			PTV			Bladder			Rectum		
	ΔV	$\Delta D_{2\%}$	$\Delta D_{98\%}$	ΔV	$\Delta D_{2\%}$	$\Delta D_{98\%}$	ΔV	ΔD_{mean}	ΔD_{2cc}	ΔV	ΔD_{mean}	ΔD_{2cc}
1												
Mean	-7.67	3.69	2.55	-6.58	3.62	-4.80	-89.28	15.78	0.88	-50.27	8.72	3.98
SD	3.25	0.32	0.42	1.71	0.27	3.76	4.60	9.57	2.74	19.18	8.38	0.27
2												
Mean	-2.58	2.83	0.86	1.38	2.74	-5.59	-39.02	2.41	2.56	-1.82	6.05	3.35
SD	1.72	0.42	0.54	1.33	0.35	3.77	31.02	3.56	0.58	10.34	3.03	0.19
3												
Mean	-6.07	3.59	0.38	2.09	3.62	-11.45	-57.79	29.37	5.82	1.43	-4.17	2.54
SD	2.97	0.31	2.07	1.41	0.32	4.78	20.32	15.06	0.27	11.01	5.97	0.52
4												
Mean	-1.63	1.07	0.00	-9.62	1.07	-0.84	-55.66	4.42	0.00	11.13	-8.90	-0.79
SD	1.39	0.66	0.41	0.96	0.64	0.97	15.34	4.98	1.56	33.86	5.62	2.62
5												
Mean	-0.41	3.50	1.50	-3.68	3.41	-8.87	-68.09	22.95	2.70	-8.31	14.36	5.12
SD	1.92	0.27	0.39	1.50	0.38	3.81	21.49	8.18	1.54	15.76	11.98	0.58
6												
Mean	-14.32	2.50	1.88	-8.78	2.51	0.48	18.55	15.74	2.89	6.84	5.64	2.84
SD	3.33	0.21	0.27	2.23	0.22	1.12	67.87	6.63	0.27	18.18	6.46	1.15
7												
Mean	-6.67	3.16	-0.83	-2.49	2.91	-7.09	-60.97	10.15	2.84	-57.76	-5.80	-2.99
SD	6.31	0.79	2.00	4.38	0.78	3.24	13.47	6.08	1.03	13.74	5.64	2.08
8												
Mean	-8.43	2.50	-2.00	-18.84	2.84	-2.91	-73.59	-3.49	-0.62	-31.31	9.92	3.25
SD	5.70	0.97	3.15	3.04	0.28	4.75	17.40	4.15	1.51	15.39	5.29	0.62
9												
Mean	-13.58	4.06	2.32	-8.34	4.00	-1.87	-85.12	10.11	1.47	-23.99	16.02	6.37
SD	1.90	0.41	0.22	1.45	0.42	1.26	6.41	5.16	1.19	6.95	7.01	0.58

CBCT, cone-beam computed tomography; CT, computed tomography; CTV, clinical target volume; PTV, planning target volume; SD, standard deviation.

change trend of the CTV and PTV in each patient was inconsistent. For example, the CTV volume of Patient 3 during treatment was smaller than the original CT image, but the PTV volume was larger than the original CT image (*Figure 3A,3B*). In this instance, we considered that the patient's organs had changed shape; the contour

difference of the CTV in the head-to-foot direction in the patient will cause this kind of situation when the CTV is expanded by Boolean operation. As the only rigid structure in this region, the femoral head has the smallest volume change with a range of -3% to 2%, mainly due to the poor image quality of CBCT compared with CT, and the edge

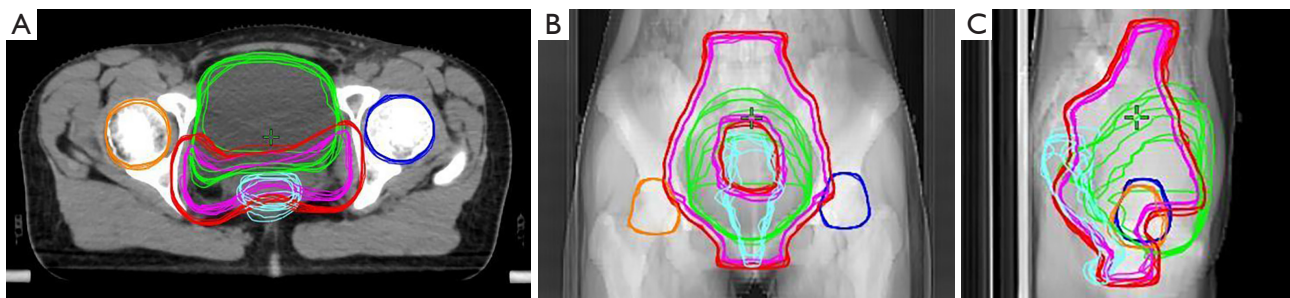


Figure 4 Contour differences in the target and OARs between fractional merged CBCT and original CT for Patient 2. (A) Cross section; (B) coronal plane; (C) sagittal plane. The magenta line is CTV, red is PTV, cyan is the rectum, green is the bladder, orange is the right femoral head, blue is the left femoral head, and the green crosshair is the positioning origin. OARs, organs at risk; CBCT, cone-beam computed tomography; CT, computed tomography; CTV, clinical target volume; PTV, planning target volume.

recognition is not clear enough. So, the humeral heads were used as a reference to correct the volume.

Changes in the shape and volume of organs in patients will bring about differences in dosimetry. Many studies have reported the necessity of adaptive strategies that consider the inter-fractional variations in bladder and rectum filling (19–21). It was found in this study that changes in the volume of the bladder and rectum had significant effects on their own D_{2cc} , and both also had significant effects on the CTV $D_{2\%}$ and PTV $D_{2\%}$ (Table 4). It can be seen from Figure 5 that all the fractional CTV $D_{2\%}$ and PTV $D_{2\%}$ doses were higher than the original plan, and the fractional PTV $D_{98\%}$ was lower than the original plan. Despite the protection of the PTV, some fractional CTV $D_{98\%}$ doses in Patients 3, 4, 7, and 8 were lower than the original plan. This indicates that differences in bladder and rectum filling, and the deformation of the target volume caused by image guidance based on CBCT bone matching, cannot guarantee the daily dose coverage of the target volume, and the homogeneity of the target volume dose deteriorates. Figure 7 shows that the rectum volume of Patient 8 was increased, and the bladder volume was significantly reduced during the 6th merged CBCT, resulting in the overall deviation of the target area toward the abdomen. When the offset distance is greater than 5 mm, the CTV breaks away from the protection of external expansion, and the dose cannot completely cover the CTV at this time. The dose homogeneity of the target area deteriorates, mainly due to tissue edema caused by treatment and gas pockets in the digestive tract that increase the density differences between tissues. Hot areas are easily formed in the air cavity area, and the increase of $D_{2\%}$ leads to uneven dose distribution. A previous study has also reported the increase in dose due to the gas pocket effect (22). These

variations in delivered doses are considered as the variation of Total Energy Released per unit Mass (TERMA) and deformations of the dose kernel in heterogeneous media. So, artifacts and cavitation affect the accuracy of CBCT-based dose calculations.

When comparing dose differences between planned doses and merged CBCT-based accumulated doses, consistent fractional dose differences resulted in significant accumulated dose differences (Table 3, Figure 6). They indicated that the $D_{2\%}$ accumulated CTV and PTV dose was higher than the original plan ($P < 0.05$), and the accumulated PTV $D_{98\%}$ was underdosed ($P < 0.05$), which were consistent with the fractional dose difference and showed a statistical difference. Although some fractional CTV $D_{98\%}$ doses were lower than the original plan, there was no statistical difference in the CTV $D_{98\%}$ between the accumulated dose and the original plan dose due to the existence of the PTV ($P > 0.05$). This work clarified that the CTV extension of 5 mm in our institution ensures the CTV dose coverage and meets the requirements of clinical treatment. For OARs, the bladder fractional dose was generally increased except for Patient 8, and the accumulated doses of the bladder D_{mean} and D_{2cc} were significantly higher than the planned dose ($P < 0.05$). This problem of bladder overdosing is not only due to patient compliance but also a reduction in urine volume during treatment because of bladder function degeneration with increased radiotherapy times (23). It showed that a small organ volume results in higher doses and larger side effects. Therefore, it is more advantageous to treat patients with a moderate bladder protocol to ensure treatment repeatability and reduce toxicity (24,25). Although there was no significant difference in the rectum D_{mean} between planned doses and merged CBCT-based accumulated doses ($P < 0.05$), the

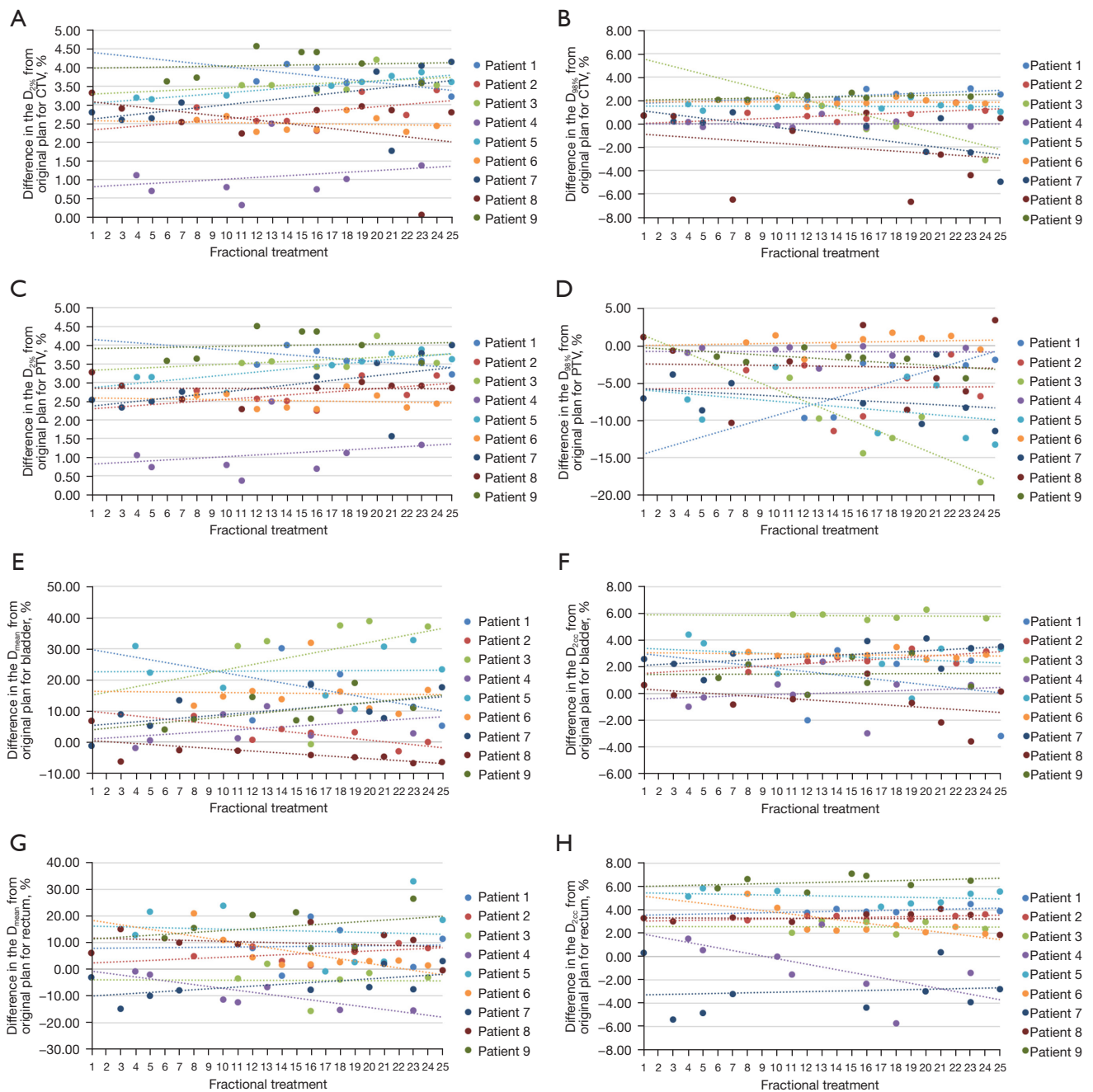


Figure 5 Fraction changes in the target and OARs during treatment: (A) CTV $D_{2\%}$; (B) CTV $D_{98\%}$; (C) PTV $D_{2\%}$; (D) PTV $D_{98\%}$; (E) Bladder D_{mean} ; (F) Bladder D_{2cc} ; (G) Rectum D_{mean} ; (H) Rectum D_{2cc} . CTV, clinical target volume; PTV, planning target volume; OARs, organs at risk.

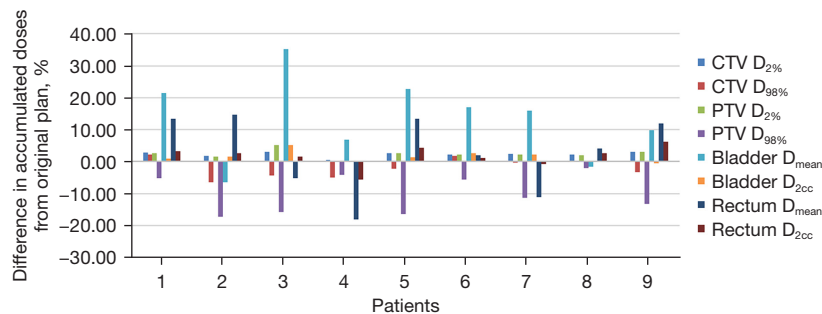
fractional rectum D_{mean} in Patients 1, 2, 5, 6, 8, and 9 was higher than that in the original plan, with a maximum of 34%. It can be seen that there is significant uncertainty in the fractional dose of IMRT for cervical cancer. ART should

be used to ensure delivery accuracy of the target volume and OARs. It can eliminate the effects of dosimetry on patient anatomic changes and gas pocket fluctuations in planning CT and treatment. ART based on periodical replanning

Table 3 Results of the dosimetric comparison for targets and OARs between planned doses and merged CBCT-based accumulated doses [M (P25, P75)]

Structure	Dose metric	Median planned dose, Gy (P25, P75)	Median accumulated dose, Gy (P25, P75)	Z value	P value
CTV	D _{2%}	48.12 (47.62, 48.16)	49.16 (48.76, 49.42)	-2.668	0.008
	D _{98%}	45.88 (45.63, 46.22)	44.70 (43.62, 46.63)	-1.820	0.069
PTV	D _{2%}	48.11 (47.60, 48.14)	49.17 (48.68, 49.49)	-2.666	0.008
	D _{98%}	44.31 (44.21, 44.58)	39.28 (37.02, 42.76)	-2.666	0.008
Bladder	D _{mean}	32.29 (31.09, 36.91)	37.78 (33.96, 43.14)	-2.310	0.021
	D _{2cc}	47.75 (46.99, 48.09)	48.45 (47.71, 48.89)	-2.100	0.036
Rectum	D _{mean}	35.63 (30.59, 37.82)	35.51 (32.80, 37.94)	-0.415	0.678
	D _{2cc}	46.70 (45.97, 47.33)	47.89 (47.17, 48.55)	-1.601	0.109

OARs, organs at risk; CBCT, cone-beam computed tomography; CTV, clinical target volume; PTV, planning target volume.

**Figure 6** The relative deviations in the target and OARs between the accumulated delivered doses and planned doses. CTV, clinical target volume; PTV, planning target volume; OARs, organs at risk.**Table 4** Effect of volume change on fractional dose delivered [r (P)]

Parameter	ΔV_{CTV} (%)	ΔV_{PTV} (%)	$\Delta V_{Bladder}$ (%)	ΔV_{Rectum} (%)
$\Delta D_{2\%, CTV}$	-0.180 (0.140)	0.299 (0.013)	-0.265 (0.028)	-0.295 (0.014)
$\Delta D_{98\%, CTV}$	-0.017 (0.893)	0.302 (0.012)	0.141 (0.247)	0.102 (0.402)
$\Delta D_{2\%, PTV}$	-0.290 (0.016)	0.173 (0.155)	-0.311 (0.009)	-0.302 (0.012)
$\Delta D_{98\%, PTV}$	-0.265 (0.028)	-0.464 (0.000)	0.225 (0.063)	0.105 (0.389)
$\Delta D_{mean, Bladder}$	-0.077 (0.528)	0.407 (0.001)	0.111 (0.364)	0.111 (0.365)
$\Delta D_{2cc, Bladder}$	-0.030 (0.804)	0.615 (0.000)	0.281 (0.019)	0.227 (0.061)
$\Delta D_{mean, Rectum}$	-0.169 (0.165)	-0.194 (0.110)	-0.181 (0.136)	-0.005 (0.968)
$\Delta D_{2cc, Rectum}$	-0.162 (0.183)	-0.103 (0.401)	-0.133 (0.275)	0.300 (0.012)

CTV, clinical target volume; PTV, planning target volume.

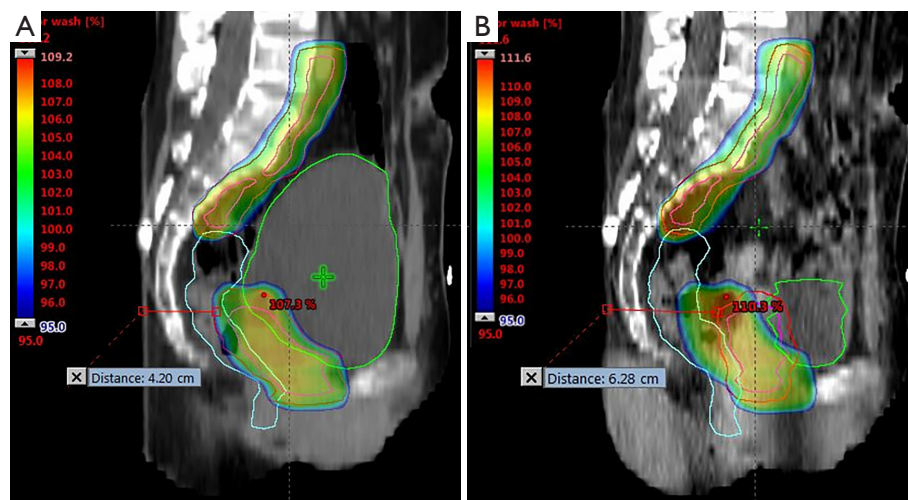


Figure 7 Example of dose distribution changes in the sagittal position for Patient 8. (A) The 95% prescription dose distribution in the original CT image. (B) The 95% prescription dose distribution in the merged CBCT image for fraction 6. The magenta line is CTV, the red line is PTV, the cyan line is the rectum, the green line is the bladder, and the green crosshair is the positioning origin. CBCT, cone-beam computed tomography; CTV, clinical target volume; PTV, planning target volume.

has been reported as beneficial for patients with various diseases (26–28).

Our work had potential limitations. The accumulated dose obtained in this study was not based on the daily CBCT; instead, we used the merged CBCT performed 1 to 2 times a week to simulate the adjacent treatment fraction status. Therefore, the difference in accumulated dose in this study cannot accurately reflect the dose change during treatment; it only provided us with a reference for the trend in accumulated dose changes in the target area and OARs. Daily imaging scans were not selected in this study because of the additional imaging dose. In clinical practice, the imaging dose in radiation therapy has traditionally been ignored due to its low magnitude and frequency compared to the therapeutic dose used to treat patients. In fact, daily imaging results in additional doses delivered to the patient. A previous study indicated that the use of a daily standard mode CBCT for a 35-fraction treatment could result in up to 1.5–2 Gy to some critical organs and an effective dose of 600 to 800 mSv to the body, which may induce an additional secondary cancer risk of 3–4% (29,30). To ensure the completeness and safety of image data acquisition, we will add an additional image dose to the treatment plan using the Monte Carlo (MC) modeling method in future studies. The MC simulation and verification of the imaging beams has been performed by Ding *et al.* using the Varian On-Board Imaging (OBI) unit (31,32).

Conclusions

In conclusion, we found that if the volume of the bladder and rectum were not strictly controlled in the radiotherapy of patients with cervical cancer, their changes were very large. Although the effect on the CTV $D_{98\%}$ was not significant, it could significantly increase the CTV $D_{2\%}$, and it will also have a significant impact on the bladder and rectum's own D_{2cc} . Therefore, more attention should be paid to the volume changes in the bladder and rectum in clinical work. Our recommendation is to perform at least CBCT once a week for organ anatomic changes monitoring plus daily verification of bladder filling with a bladder scan (24). Finally, the merged CBCT data in this study provides a suitable approach in ART that may be useful clinically to respond to the daily anatomy variations in cervical cancer patients. It offers a good possibility for evaluating the daily applied dose for the bladder and rectum.

Acknowledgments

Funding: This study was supported by the Chongqing Natural Science Foundation of China (No. cstc2021jcyj-msxmX0441) and the Joint Project of Chongqing Health Commission and Science and Technology Bureau (No. 2022DBXM005).

Footnote

Reporting Checklist: The authors have completed the MDAR reporting checklist. Available at <https://atm.amegroups.com/article/view/10.21037/atm-22-6157/rc>

Data Sharing Statement: Available at <https://atm.amegroups.com/article/view/10.21037/atm-22-6157/dss>

Conflicts of Interest: All authors have completed the ICMJE uniform disclosure form (available at <https://atm.amegroups.com/article/view/10.21037/atm-22-6157/coif>). The authors have no conflicts of interest to declare.

Ethical Statement: The authors are accountable for all aspects of the work in ensuring that questions related to the accuracy or integrity of any part of the work are appropriately investigated and resolved. The study was conducted in accordance with the Declaration of Helsinki (as revised in 2013). This study was approved by the Ethics Committee of Chongqing University Cancer Hospital (No. CZLS2021048-A) and informed consent was taken from all the patients.

Open Access Statement: This is an Open Access article distributed in accordance with the Creative Commons Attribution-NonCommercial-NoDerivs 4.0 International License (CC BY-NC-ND 4.0), which permits the non-commercial replication and distribution of the article with the strict proviso that no changes or edits are made and the original work is properly cited (including links to both the formal publication through the relevant DOI and the license). See: <https://creativecommons.org/licenses/by-nc-nd/4.0/>.

References

1. Wang Y, Ballo MT, Hubler A, et al. Intensity-Modulated Versus Three-Dimensional Conformal Radiotherapy for Cervical Cancer: National Trend and Survival. *Int J Radiat Oncol* 2019;105:E339-40.
2. Marjanovic D, Plesinac Karapandzic V, Stojanovic Runic S, et al. Acute toxicity of postoperative intensity-modulated radiotherapy and three-dimensional conformal radiotherapy for cervical cancer: The role of concomitant chemotherapy. *J BUON* 2019;24:2347-54.
3. Wortman BG, Post CCB, Powell ME, et al. Radiation Therapy Techniques and Treatment-Related Toxicity in the PORTEC-3 Trial: Comparison of 3-Dimensional Conformal Radiation Therapy Versus Intensity-Modulated Radiation Therapy. *Int J Radiat Oncol Biol Phys* 2022;112:390-9.
4. Gort EM, Beukema JC, Matysiak W, et al. Interfraction motion robustness and organ sparing potential of proton therapy for cervical cancer. *Radiother Oncol* 2021;154:194-200.
5. Tsujii K, Ueda Y, Isono M, et al. Dosimetric impact of rotational setup errors in volumetric modulated arc therapy for postoperative cervical cancer. *J Radiat Res* 2021;62:688-98.
6. Niedzielski JS, Liu Y, Ng SSW, et al. Dosimetric Uncertainties Resulting From Interfractional Anatomic Variations for Patients Receiving Pancreas Stereotactic Body Radiation Therapy and Cone Beam Computed Tomography Image Guidance. *Int J Radiat Oncol Biol Phys* 2021;111:1298-309.
7. de Crevoisier R, Lafond C, Mervoyer A, et al. Image-guided radiotherapy. *Cancer Radiother* 2022;26:34-49.
8. Tan Mbbs Mrcp Frcr Md LT, Tanderup PhD K, Kirisits PhD C, et al. Image-guided Adaptive Radiotherapy in Cervical Cancer. *Semin Radiat Oncol* 2019;29:284-98.
9. Kong V, Hansen VN, Hafeez S. Image-guided Adaptive Radiotherapy for Bladder Cancer. *Clin Oncol (R Coll Radiol)* 2021;33:350-68.
10. Nabavizadeh N, Elliott DA, Chen Y, et al. Image Guided Radiation Therapy (IGRT) Practice Patterns and IGRT's Impact on Workflow and Treatment Planning: Results From a National Survey of American Society for Radiation Oncology Members. *Int J Radiat Oncol Biol Phys* 2016;94:850-7.
11. Utena Y, Takatsu J, Sugimoto S, et al. Trajectory log analysis and cone-beam CT-based daily dose calculation to investigate the dosimetric accuracy of intensity-modulated radiotherapy for gynecologic cancer. *J Appl Clin Med Phys* 2021;22:108-17.
12. Feng Z, Wu H, Zhang Y, et al. Dosimetric comparison between jaw tracking and static jaw techniques in intensity-modulated radiotherapy. *Radiat Oncol* 2015;10:28.
13. Kim JI, Park JM, Park SY, et al. Assessment of potential jaw-tracking advantage using control point sequences of VMAT planning. *J Appl Clin Med Phys* 2014;15:4625.
14. Wu H, Jiang F, Yue H, et al. A comparative study of identical VMAT plans with and without jaw tracking technique. *J Appl Clin Med Phys* 2016;17:133-41.
15. Hu CC, Huang WT, Tsai CL, et al. Practically acquired and modified cone-beam computed tomography images for accurate dose calculation in head and neck cancer.

- Strahlenther Onkol 2011;187:633-44.
16. Ding S, Liu H, Wang B, et al. Inter- and Intrafraction Bladder and Rectum Motion in Patients With Cervical Cancer Under MR-Guided Radiotherapy on a 1.5T MR-Linac. *Int J Radiat Oncol* 2021;111:e612.
 17. Li X, Wang L, Cui Z, et al. Online MR evaluation of inter- and intra-fraction uterus motions and bladder volume changes during cervical cancer external beam radiotherapy. *Radiat Oncol* 2021;16:179.
 18. Jadon R, Pembroke CA, Hanna CL, et al. A systematic review of organ motion and image-guided strategies in external beam radiotherapy for cervical cancer. *Clin Oncol (R Coll Radiol)* 2014;26:185-96.
 19. Felici F, Benkreira M, Lambaudie É, et al. Adaptive Magnetic Resonance-Guided External Beam Radiation Therapy for Consolidation in Recurrent Cervical Cancer. *Adv Radiat Oncol* 2022;7:100999.
 20. Zhang Y, Zhang X, Li J, et al. Analysis of the Influence of Peripheral Anatomical Changes for CBCT-Guided Prostate Cancer Radiotherapy. *Technol Cancer Res Treat* 2021;20:15330338211016370.
 21. van de Schoot AJAJ, de Boer P, Visser J, et al. Dosimetric advantages of a clinical daily adaptive plan selection strategy compared with a non-adaptive strategy in cervical cancer radiation therapy. *Acta Oncol* 2017;56:667-74.
 22. Fidanzio A, Porcelli A, Azario L, et al. Quasi real time in vivo dosimetry for VMAT. *Med Phys* 2014;41:062103.
 23. Pearson D, Gill SK, Campbell N, et al. Dosimetric and volumetric changes in the rectum and bladder in patients receiving CBCT-guided prostate IMRT: analysis based on daily CBCT dose calculation. *J Appl Clin Med Phys* 2016;17:107-17.
 24. Luo H, Jin F, Yang D, et al. Interfractional variation in bladder volume and its impact on cervical cancer radiotherapy: Clinical significance of portable bladder scanner. *Med Phys* 2016;43:4412.
 25. Jin F, Luo HL, Zhou J, et al. A parameterized model for mean urinary inflow rate and its preliminary application in radiotherapy for cervical cancer. *Sci Rep* 2017;7:280.
 26. Roberts HJ, Huynh E, Williams CL, et al. Impact of Stereotactic MR-Guided Adaptive Radiation Therapy on Early Clinical and Dosimetric Outcomes in Patients With Pancreatic Cancer. *Int J Radiat Oncol* 2021;111:e72.
 27. Avgousti R, Antypas C, Armpilia C, et al. Adaptive radiation therapy: When, how and what are the benefits that literature provides? *Cancer Radiother* 2022;26:622-36.
 28. Dial C, Weiss E, Siebers JV, et al. Benefits of adaptive radiation therapy in lung cancer as a function of replanning frequency. *Med Phys* 2016;43:1787.
 29. Alaei P, Spezi E. Imaging dose from cone beam computed tomography in radiation therapy. *Phys Med* 2015;31:647-58.
 30. Kan MW, Leung LH, Wong W, et al. Radiation dose from cone beam computed tomography for image-guided radiation therapy. *Int J Radiat Oncol Biol Phys* 2008;70:272-9.
 31. Ding GX, Coffey CW. Beam characteristics and radiation output of a kilovoltage cone-beam CT. *Phys Med Biol* 2010;55:5231-48.
 32. Ding GX, Duggan DM, Coffey CW. Accurate patient dosimetry of kilovoltage cone-beam CT in radiation therapy. *Med Phys* 2008;35:1135-44.
- (English Language Editor: D. Fitzgerald)

Cite this article as: Yang H, Zhao X, He Y, Tan X, Peng H, Zhong M, Li Q, Liu X, He Y, Luo H, Jin F. Dosimetric impacts of cone-beam computed tomography (CBCT)-based anatomic changes in intensity-modulated radiotherapy for cervical cancer. *Ann Transl Med* 2022;10(24):1381. doi: 10.21037/atm-22-6157